33

Using Magnetic Fields and Storing Data

CHAPTER PREVIEW

If you were asked to give an example of a magnetic material instinctively you would probably say iron. It is a good example, but in its pure form iron is not a very useful magnet. Ceramics can be magnetic too and they were the first magnets known to humans. About 600,000 t of ceramic magnets are produced each year making them, in terms of volume, commercially more important than metallic magnets. The largest market segment is hard ferrites (permanent magnets) that are used in a range of applications including motors for electric toothbrushes and windshield wipers in automobiles, refrigerator door seals, speakers, and stripes on the back of the ubiquitous credit and ATM cards. Soft ferrites can be magnetized and demagnetized easily and are used in cell telephones, transformer cores, and, now to a somewhat lesser extent, magnetic recording.

Ferrite is a term used for ceramics that contain Fe_2O_3 as a principal component.

Magnetism has probably fascinated more people, including Socrates and Mozart (listen to *Così fan tutte*), over the years than any other materials property. For over four thousand years the strange power of magnets has captured our imagination. Yet it remains the least well understood of all properties. In this chapter we will start by describing some of the basic characteristics of magnetic materials, which often contain one of the first row transition metals, Fe, Co, or Ni. The electron arrangement in the 3d level of these atoms is the key. The manganates are a very interesting class of magnetic ceramic. Although they are not new, the recent discovery that they exhibit colossal magnetoresistance (just like the giant magnetoresistance observed in metal multilayers only *much* bigger) has renewed interest in these materials. Structurally the manganates are very similar to the high-temperature superconductors (HTSCs). The similarity may be more than coincidental.

33.1 A BRIEF HISTORY OF MAGNETIC CERAMICS

Applications of magnetism began with ceramics. The first magnetic material to be discovered was lodestone, which is better known now as magnetite (Fe_3O_4). In its naturally occurring state it is permanently magnetized and is the most magnetic mineral. The strange power of lodestone was well known in ancient times. In c. 400 BCE Socrates dangled iron rings beneath a piece of lodestone and found that the lodestone enabled the rings to attract other rings. They had become magnetized. Even earlier (~c. 2600 BCE) a Chinese legend tells of the Emperor Hwang-ti being guided into battle through a dense fog by means of a small pivoting figure with a piece of lodestone embedded in its outstretched arm. The figure always pointed south and was probably the first compass. The term lodestone was coined by the British from the old English word *lode*, which meant to *lead* or *guide*.

Figure 33.1 shows an ancient Chinese compass. The spoon or ladle was carved out of lodestone and rests on a polished bronze plate. The rounded bottom of the spoon swivels on the plate until it points south. Although this compass has been found to work it was used apparently for quasimagical rather than navigational purposes.

Magnetite is found in many parts of the world and is an important iron ore used for steel making. The word *magnet* comes from the Greek word *magnes*, which itself may derive from the ancient colony of Magnesia (in Turkey). Magnetite was mined in Magnesia 2500 years ago. Today, large deposits of magnetite are found at Kiruna in Sweden and in the Adirondack region of New York.

Commercial interest in ceramic magnets really started in the early 1930s with the filing of a Japanese patent describing applications of copper and cobalt ferrites. In 1947 J.L. Snoeck of N.V. Philips Gloeilampenfabrieken performed a detailed study of ferrites, and the following year Louis Néel published his theory of ferrimagnetism. This latter study was particularly important because most of the ceramics that have useful magnetic properties are ferrimagnetic. The first commercial ceramic magnets were produced in 1952 by researchers at the Philips Company,

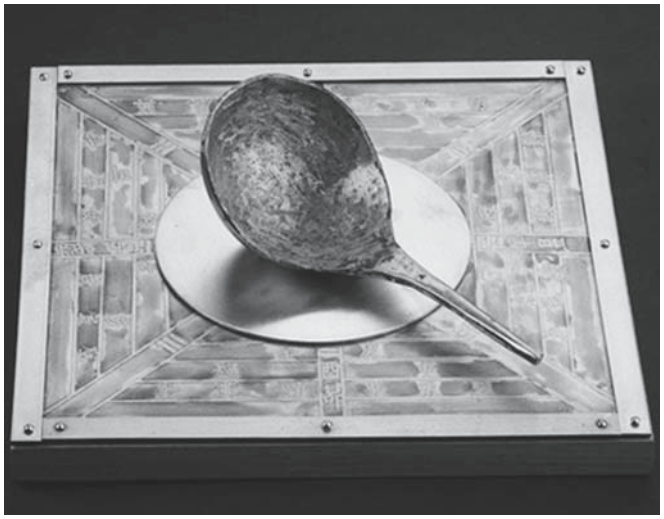

FIGURE 33.1 An ancient Chinese compass.

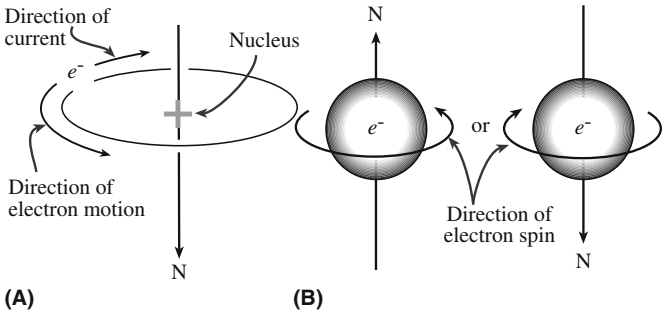

FIGURE 33.2 Generation of atomic magnetic moments by (a) electron orbital motion around the nucleus; (b) electron spin around its axis of rotation.

the same company that introduced the compact audiocassette in 1963.

33.2 MAGNETIC DIPOLES

The Danish physicist Hans Christian Oersted discovered that an electric current (i.e., moving electrons) gives rise to a magnetic force. In an atom, there are two possible sources of electron motion that can create a magnetic dipole and produce the resultant macroscopic magnetic properties of a material. Magnetic dipoles are small internal magnets with north and south poles.

MAGNETIC MOMENTS

The fundamental magnetic moment is the Bohr magneton, μ_B, which has a value of $9.27 \times 10^{-24}\,A{\cdot}m^2$.

The orbital magnetic moment, μ_{orb}, of a single electron is

$$\mu_{orb} = \mu_B \sqrt{[l(l+1)]} \qquad \text{(Box 33.1)}$$

l is the orbital shape quantum number (see Chapter 3).

The spin magnetic moment of an electron is

$$\mu_s = 2\mu_B \sqrt{[m_s(m_s+1)]} \qquad \text{(Box 33.2)}$$

In ceramics where the magnetic behavior is due to the presence of transition metal ions with unpaired electron spins in the 3d orbital the magnetic moment of the ion due to electron spin, μ_{ion}, is

$$\mu_{ion} = 2\mu_B \sqrt{[S(S+1)]} \qquad \text{(Box 33.3)}$$

$$S = \sum m_s$$

- *Orbital motion*. Equivalent to a small current loop generating a very small magnetic field. The direction of the magnetic moment is along the orbit axis as illustrated in Figure 33.2a.
- *Spin*. Origin of the fourth quantum number, m_s, that we used in Chapter 3. The magnetic moment is along the spin axis as shown in Figure 33.2b and will be either up ($m_s = +1/2$) or in an antiparallel down direction ($m_s = -1/2$).

The magnetic moment due to electron spin is, when present, dominant

TABLE 33.1 Magnetic Moments of Isolated Transition Metal Cations

Cations	*Electronic configuration*	*Calculated moments using Eq. B3*	*Measured moments (μ_B)*
Sc^{3+}, Ti^{4+}	$3d^0$	0.00	0.0
V^{4+}, Ti^{3+}	$3d^1$	1.73	1.8
V^{3+}	$3d^2$	2.83	2.8
V^{2+}, Cr^{3+}	$3d^3$	3.87	3.8
Mn^{3+}, Cr^{2+}	$3d^4$	4.90	4.9
Mn^{2+}, Fe^{3+}	$3d^5$	5.92	5.9
Fe^{2+}	$3d^6$	4.90	5.4
Co^{2+}	$3d^7$	3.87	4.8
Ni^{2+}	$3d^8$	2.83	3.2
Cu^{2+}	$3d^9$	1.73	1.9
Cu^{+}, Zn^{2+}	$3d^{10}$	0.00	0.0

TABLE 33.2 Terms and Units Used in Magnetism

Parameter	*Definition*	*Units/value*	*Conversion factor*
H	Magnetic field strength	A/m	$1\,A/m = 4\pi \times 10^{-3}$ oersted (Oe)
H_c	Coercive field	A/m	
H_{cr}	Critical field	A/m	
M	Magnetization	A/m	
B	Magnetic flux density Magnetic induction	T	$T = Wb\,m^{-2} = kg\,A^{-1}\,s^2 = V\,s\,m^{-2}$ $= 10^4$ gauss (G)
μ_o	Permeability of a vacuum	$4\pi \times 10^{-7}$ H/m	$1\,H = 1\,J\,s^2\,C^{-2}$
μ	Permeability	H/m	$1\,H/m = 1\,Wb\,m^{-1}\,A^{-1}$
μ_r	Relative permeability	Dimensionless	
χ	Susceptibility	Dimensionless	
μ_{ion}	Net magnetic moment of an atom or ion	$A \cdot m^2$	
μ_s	Spin magnetic moment	$A \cdot m^2$	
μ_{orb}	Orbital magnetic moment	$A \cdot m^2$	
μ_B	Bohr magneton	$9.274 \times 10^{-24}\,A \cdot m^2$	
θ_c	Curie temperature	K	$0\,K = -273°C$
θ_N	Néel temperature	K	
T_c	Critical temperature for superconductivity	K	
C	Curie constant	K	

over that due to orbital motion. Table 33.1 lists values of μ_{ion} calculated for some first row transition metal ions using Eq. Box 33.3. You can see that, in general, the calculated values agree well with the experimental values. This agreement shows that we are justified in considering only the contribution of the spin magnetic moment to the overall magnetic moment.

When an electron orbital in an atom is filled, i.e., all the electrons are paired up, both the orbital magnetic moment and the spin magnetic moment are zero.

33.3 THE BASIC EQUATIONS, THE WORDS, AND THE UNITS

Table 33.2 lists the important parameters used in this chapter and their units. The situation regarding units is more complicated for magnetism than for almost any other property. The reason is that some of the older units, in particular the oersted (Oe) and the gauss (G), are still in widespread use despite being superceded, in the SI system, by A/m and T, respectively.

The properties of most interest to us in the description of magnetic behavior are

- μ
- χ

These terms are, of course, related to each other and by considering the role of H to macroscopic measures such as M and B.

The usual starting point to arrive at expressions for μ and χ is to consider a coil of wire in a vacuum as illustrated in Figure 33.3a. A current, I, passed through the wire generates a magnetic field H

$$H = IN \tag{33.1}$$

where N is the number of turns of wire per meter. The magnetic induction or magnetic flux density, B, is related to H by

$$B = \mu_0 H \tag{33.2}$$

μ_o is a universal constant.

When a material is placed inside the coil, as shown in Figure 33.3b, it becomes "magnetized." The magnetic

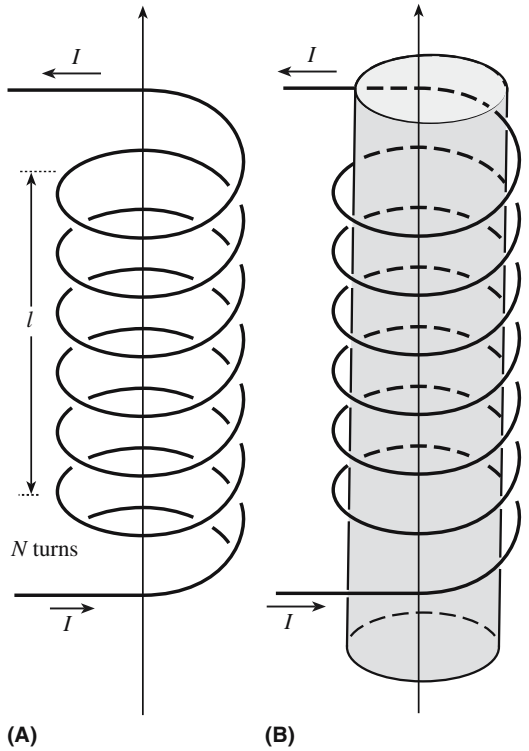

FIGURE 33.3 Generation of a magnetic field by current flowing in a coil of wire (a) in a vacuum; (b) with a material present.

moment produced in the material by the external field changes B:

$$B = \mu_0 H + \mu_0 M \tag{33.3}$$

M represents the response of the material to H, which is linear, and the ratio gives

$$\chi = M/H \tag{33.4}$$

By simple substitution we get

$$B = \mu_0(1 + \chi)H \tag{33.5}$$

B/H is then the permeability:

$$B/H = \mu_0(1 + \chi) = \mu \tag{33.6}$$

The ratio of the permeabilities gives us the relative permeability:

$$\frac{\mu}{\mu_0} = 1 + \chi = \mu_r \tag{33.7}$$

There are many qualitative similarities between magnetic parameters and those we used to describe dielectrics in Chapter 31. In the former case, the material is responding to an applied magnetic field, and in the latter case, it is responding to an applied electric field.

χ AND μ

Susceptibilities are generally used when the response to an applied magnetic field is weak (of interest only to physicists!). Permeabilities are used when the response is large—of great interest to engineers!

- H and the electric field strength ξ (V/m). Both are the external driving force, which causes the orientation of either magnetic or electric dipoles resulting in magnetization or polarization, respectively.
- B and the polarization P (C/m^2). Both correspond to the total field after dipole orientation.
- χ and dielectric constant, κ. Both are dimensionless "constants" that describe the magnitude of a material's response to the applied field. They are both properties of a material and depend on the types of atoms, the interatomic bonding, and, the crystal structure.
- μ_o and the permittivity of a vacuum ε_0 *are* constants. They are reference values to establish the strength of a materials response to H or ξ, respectively.

The similarities described above are not surprising. In both cases, we are concerned with the relationship between an external field and the dipoles within a material. Despite these similarities the physical nature of the dipoles and their origin is very different. In the case of a dielectric, the dipoles are electric; there is a separation of positive and negative charges. These dipoles can be permanent or induced. In a magnetic material, the dipoles are, of course, magnetic in origin and are due to electron motion.

A note on terminology: In most materials science textbooks, as we have done here, H is defined as the magnetic field or the applied magnetic field and B as the magnetic flux density. In many physics textbooks B is referred to as the magnetic field and H is often ignored. The physics convention is adopted for purely historical reasons, but it does have the advantage of reducing the number of terms we need to consider. Also H has nothing to do with a material whereas B is a measure of the response of a material to an applied magnetic field. Another point to note is that B and H are both vector quantities and because the magnetic properties of a material are anisotropic (different along different directions in the crystal) they should actually be represented by a second-rank tensor.

MAXWELL EQUATIONS

The magnetic, electric, and optical properties of a material are all related mathematically through the Maxwell equations.

33.4 THE FIVE CLASSES OF MAGNETIC MATERIAL

There are five main types of magnetic behavior and these can be divided into two general categories:

- Induced
- Spontaneous

Table 33.3 summarizes the properties of the five classes. We can find examples of each in ceramics.

33.5 DIAMAGNETIC CERAMICS

Most ceramics are diamagnetic. The reason is that all the electrons are paired during bond formation and as a result the net magnetic moment due to electron spin is zero. Table 33.4 lists χ for several diamagnetic materials. Cu, Au, and Ag are diamagnetic even though their atoms have unpaired valence electrons. When the atoms combine to form the metal the valence electrons are shared by the crystal as a whole (to form the electron gas) and, on average, there will be as many electrons with $m_s = +1/2$ as with $m_s = -1/2$.

Most diamagnetic ceramics are of no commercial significance and of little scientific interest, at least not for their magnetic behavior. The one exception is the ceramic superconductors, which are perfect diamagnets below a critical magnetic field.

TABLE 33.3 Magnetic Classification of Materials

Class	*Critical temperature*	χ	*Temperature variation of* χ	*Spontaneous magnetization*	*Structure on atomic scale*
Diamagnetic	None	-10^{-6} to -10^{-5}	Constant	None	Atoms have no permanent dipole moments
Paramagnetic	None	$+10^{-5}$ to $+10^{-3}$	$\chi = C/T$	None	Atoms have permanent dipole moments; neighboring moments do not interact
Ferromagnetic	θ_C	Large (below θ_C)	Above θ_C, $\chi = C/(T - \theta)$, with $\theta \approx \theta_C$	Below θ_C, $M_s(T)/M_s(0)$ against T/θ_C follows a universal curve; above θ_C, none	Atoms have permanent dipole moments; interaction produces parallel alignment
Antiferromagnetic	θ_N	As paramagnetic	Above θ_N, $\chi = C/(T \pm \theta)$, with $\theta \neq \theta_N$, below θ_N, χ decreases, anisotropic	None	Atoms have permanent dipole moments; interaction produces antiparallel alignment
Ferrimagnetic	θ_C	As ferromagnetic	Above θ_C, $\chi \approx C/(T \pm \theta)$, with $\theta \neq \theta_C$	Below θ_C, does not follow universal curve; above θ_C, none	Atoms have permanent dipole moments; interaction produces antiparallel alignment; moments are not equal

33.6 SUPERCONDUCTING MAGNETS

When a superconductor in its normal (i.e., nonsuperconducting) state is placed in a magnetic field and then cooled below its critical temperature the induced magnetization, M, exactly opposes H and so from Eq. 33.3, we can write

$$B = 0 \qquad (33.8)$$

LONDON PENETRATION DEPTH

Although there is no magnetic field in the bulk of a superconductor it does penetrate below the surface to a depth of between 0.2 and 0.8 μm.

CRITICAL MAGNETIC FIELDS FOR YBCO

H_{c1} (T)	$\parallel c$ ~0.1	$\parallel a,b$ ~0.01
H_{c2} (T)	$\parallel c$ ~50	$\parallel a,b$ ~200

$\parallel c$ field along the c axis of the unit cell
$\parallel a,b$ field in the basal plane
These H_{c2} values are enormous. The world's most powerful magnet is about 40 T.

The net effect is that the whole of the magnetic flux appears to have been suddenly ejected from the material and it behaves as a perfect diamagnet. This phenomenon is known as the Meissner effect and is usually demonstrated by suspending a magnet above a cooled pellet of the superconductor.

There is an upper limit to the strength of the magnetic field that can be applied to a superconductor without changing its diamagnetic behavior. At a critical field H_{cr} the magnetization goes toward zero and the material reverts to its normal state. For most elemental superconductors M rises in magnitude up to H_{cr} and then abruptly drops to zero; this is Type I behavior.

A few elemental and most compound superconductors, including all HTSCs, exhibit Type II behavior. Above a certain field, H_{c1}, magnetic flux can penetrate the material without destroying superconductivity. Then at a (usually much) higher field, H_{c2}, the material reverts to the normal state. These two behaviors are compared in Figure 33.4.

When a Type II superconductor is in the "mixed" state it consists of both normal and superconducting regions. The normal regions are called vortices, which are arranged parallel to the direction of the applied field. At low temperature the vortices are in a close-packed arrangement and vibrate about their equilibrium positions, in the same way that atoms in a solid vibrate. If the temperature is high enough the vortex motion becomes so pronounced that the

TABLE 33.4 Magnetic Susceptibilities for Several Diamagnetic Materials

Material	χ *(ppm)*
Al_2O_3	−37.0
Be	−9.0
BeO	−11.9
Bi	−280.1
B	−6.7
CaO	−15.0
CaF_2	−28.0
C (diamond)	−5.9
C (graphite)	−6.0
Cu	−5.5
Ge	−76.8
Au	−28.0
Pb	−23.0
LiF	−10.1
MgO	−10.2
Si	−3.9
Ag	−19.5
NaCl	−30.3

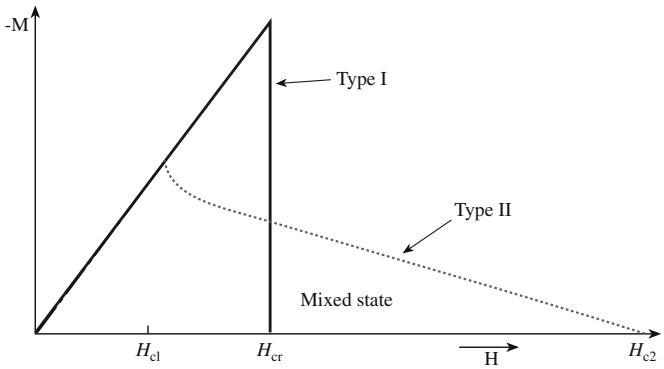

FIGURE 33.4 Magnetization behavior of Type I and Type II superconductors as a function of the applied field.

TABLE 33.5 Magnetic Susceptibilities for Several Paramagnetic Materials

Material	χ *(ppm)*
Al	+16.5
Ca	+40.0
Ce	+2450
CeO_2	+26.0
Cr	+180
Cr_2O_3	+1965
Li	+14.2
Mg	+13.1
Na	+16.0
Ti	+153.0
TiO_2	+5.9

arrangement randomizes and the vortex lattice "melts." Defects in the material can trap or pin vortices in place and higher temperatures are then needed to cause "melting." Pinning is of considerable practical importance because it enables higher currents to flow through the material before superconductivity is lost.

One of the most exciting potential applications of the Meissner effect is magnetic levitation (maglev) for advanced high-speed transportation. Pilot maglev trains that can reach speeds of more than 550 km/h have already been developed in Japan, and other countries have plans to develop maglev train services. The first U.S. maglev train was scheduled for the campus of Old Dominion University in Virginia with plans to complete construction by 2003. But the project has suffered a continuation of major setbacks since then.

Although ceramic superconductors have not been used for the generation of large magnetic fields, because it is difficult to form them into long wires, they have been made into superconducting quantum interference devices (SQUIDs). The essential component of a SQUID is the Josephson junction, a thin (~1 nm) insulating layer between two superconductors through which weak supercurrents consisting of Cooper pairs can tunnel without an applied voltage. The insulating barrier can be a deposited thin film or, in the case of some of the ceramic superconductors, a high-angle grain boundary (GB), such as that shown in Figure 14.37, which works well.

A SQUID can be used to detect very small (~10^{-15} T) changes in B. When a Josephson junction is exposed to a magnetic field steps are produced in the I–V behavior. This is similar to what happens when the junction is irradiated with microwaves (as we showed in Chapter 30). Each step corresponds to a quantum change in B. Uses for SQUIDs include the following:

- They can detect small changes in magnetic field strength at the earth's surface that can then be related to the underlying geological structure (e.g., thickness of the crust, movement of magnetic poles over time, etc.).
- Magnetic imaging using scanning SQUID microscopy. This allows local magnetic fields to be measured at the surface of a sample.
- Searching for submarines. When a submarine moves through the water, the metal hull slightly disturbs the earth's magnetic field and this small distortion can be measured.
- The human brain can be imaged by detecting small magnetic fields produced as a result of the currents due to neural activity. This area of research is called magnetoencephalography (MEG) and is being used to study epilepsy.

REFERENCE POINTS

$B = 10^{-12}$ T at the Earth's surface.

The human body produces a magnetic field of ~10^{-10} T.

33.7 PARAMAGNETIC CERAMICS

The magnetic moment is due to unpaired electron spins. Magnetic susceptibilities are positive as shown in Table 33.5, because the magnetic moments line up with H and this leads to an increase in B. However, adjacent magnetic dipoles essentially behave independently; there is no interaction between them. It is this lack of an interaction that separates paramagnetic materials from ferromagnets.

Most first row transition metals, e.g., Ti and Cr, are paramagnetic because they have unpaired electrons in their 3d orbitals (see Table 33.1). The number of unpaired electrons per atom is determined using Hund's rule (Section 3.5).

Nontransition metals, e.g., Na, may be paramagnetic due to the alignment of the spin moment of some of the valence electrons with the applied field. This effect, known as Pauli paramagnetism, is much weaker than that due to unpaired 3d electrons and involves electrons moving into a higher energy level and changing their spin direction. This process can happen only if the gain in magnetic

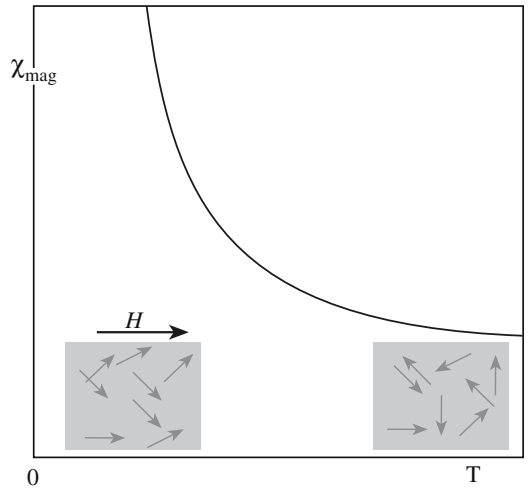

FIGURE 33.5 Schematic showing how χ varies with T for a paramagnetic solid. The insets indicate the direction of the magnetic dipoles in the solids.

energy is more than the energy needed for electron promotion. Some oxides containing transition metal or rare earth ions, such as CeO_2 and Cr_2O_3, are also paramagnetic.

The temperature dependence of paramagnetic susceptibility is shown in Figure 33.5 and follows the Curie law:

$$\chi = \frac{C}{T} \tag{33.9}$$

There are currently no commercial applications for paramagnetism.

33.8 MEASURING χ

The most straightforward way to obtain χ is the classical Gouy method. The material, in the form of a rod, is attached to one arm of a sensitive balance. It is then placed between the poles of a magnet. If the sample is paramagnetic its energy is lower when it is inside the magnetic field, and so there is a force, F, drawing it into the field. If the sample is diamagnetic its energy is less if it is outside the field, and so F is in the opposite direction.

Qualitatively the sign of χ can be determined by whether the force on the sample (the apparent weight change measured by the balance) is positive or negative. We can quantify the value of χ using Eq. 33.10:

$$F = \frac{1}{2} A\chi H^2 \tag{33.10}$$

where A is the cross-sectional area of the sample.

Other methods can be used to determine magnetization and susceptibility, but all rely either on measuring the force exerted on the sample by the magnetic field (as in the Gouy method) or on detecting currents induced in a circuit placed close to the magnetic material. The main disadvantage of the Gouy method is that it requires quite a large sample (~ grams).

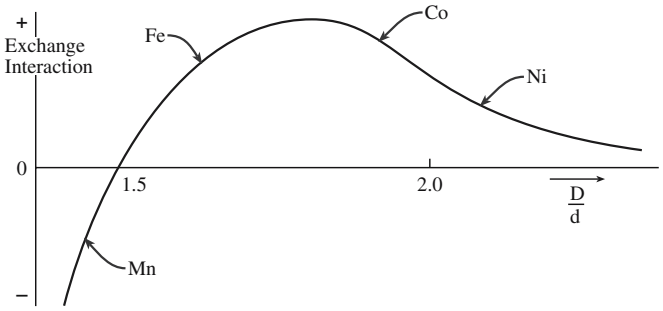

FIGURE 33.6 The Slater–Bethe curve showing the magnitude and sign of J as a function of D/d.

33.9 FERROMAGNETISM

The origin of ferromagnetism, like paramagnetism, is the presence of unpaired electron spins. However, in a ferromagnetic material there is an interaction between adjacent dipoles. Of the first row transition metals only Fe, Co, and Ni are ferromagnetic. So why is Cr paramagnetic not ferromagnetic? The reason is due to a quantum mechanical exchange interaction between the 3d orbitals on adjacent atoms, which is represented mathematically by the exchange integral, J. If $J > 0$ there is an interaction between adjacent magnetic dipoles causing them to line up and the material is ferromagnetic (below the Curie temperature, θ_c). If $J < 0$ adjacent dipoles are antiparallel and the material is antiferromagnetic (below the Néel temperature, θ_N).

The magnitude and the size of J depend on the interatomic separation, D, and the diameter, d, of the electron orbital under consideration as shown in Figure 33.6 (the Slater–Bethe curve) for the case of the 3d orbitals of Fe, Co, and Ni.

D can be determined simply by looking up the atomic radius of the element and doubling it, e.g., for Fe r = 0.124 nm and D = 0.248 nm. The value of d can be estimated using Eq. Box 3.2 in Section 3.2. For the 3d orbitals of Fe r = 0.159 nm. Hence D/d is 1.56, as shown in Figure 33.6. J is more difficult to determine. It is related to the overlap of the electron orbitals and involves integrating the products of the wavefunctions for the electron orbitals on adjacent atoms.

If there is significant overlap of the 3d orbitals then, by the requirements of the Pauli exclusion principle, the spins must be antiparallel ($J < 0$). If the separation is too large then

MEASURING χ

It is important to determine χ to know if a material is a superconductor. Having a very low electrical resistivity or an abrupt drop in resistivity is not a defining criterion. A strong magnet has a large value of χ.

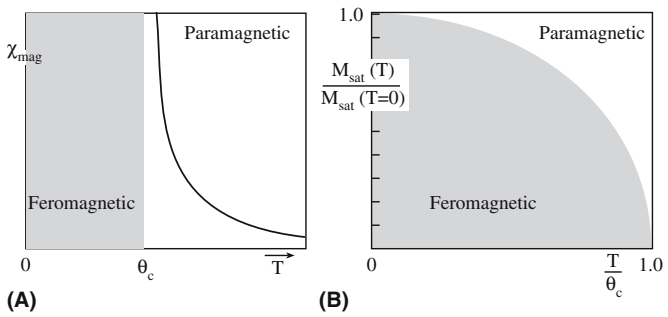

FIGURE 33.7 Schematic showing how (a) χ varies with T; (b) M varies with T for a ferromagnet.

there is no appreciable interaction. However, in the case of iron, cobalt, and nickel the exchange interaction is large and positive and the electron spins are parallel.

The magnetic susceptibility of a ferromagnetic material varies with temperature (Figure 33.7a) according to the Curie–Weiss law:

$$\chi = C/(T - \theta_c) \tag{33.11}$$

You will recognize this type of variation as being very similar to an order–disorder transition. Above θ_c the material become paramagnetic because of randomization of the spin magnetic moments. M decreases from its maximum value at 0 K and vanishes at θ_c as shown in Figure 33.7(b).

Chromium dioxide (CrO_2) is at present the most important ferromagnetic ceramic. It is used as magnetic media in audio and video recording tapes. In this application, the CrO_2 is not in the pure form but is usually doped to improve its properties.

CrO_2 has the rutile (TiO_2) structure (Figure 6.11). The Cr^{4+} ions are located at the corners of the unit cell and there is a distorted CrO_6 octahedron in the center. The lattice parameters are $a = 0.437$ nm and $c = 0.291$ nm. CrO_2 does not occur in nature and is usually manufactured by thermal decomposition of CrO_3 at ~500°C under high pressure (>200 MPa) in the presence of water.

33.10 ANTIFERROMAGNETISM AND COLOSSAL MAGNETORESISTANCE

In an antiferromagnet there is exact cancellation of the magnetic moments. We can think of an antiferromagnetic material as consisting of two ferromagnetic lattices in which the spin magnetic moments are equal in magnitude but opposite in direction. Above θ_N the antiferromagnetic spin alignments are randomized and the material becomes paramagnetic. The temperature dependence of the magnetic susceptibility is shown in Figure 33.8.

The following oxides are antiferromagnetic:

$$\text{MnO } (\theta_N = 122\,\text{K}) \qquad \text{NiO } (\theta_N = 523\,\text{K})$$
$$\text{CoO } (\theta_N = 293\,\text{K}) \qquad \text{FeO } (\theta_N = 198\,\text{K})$$

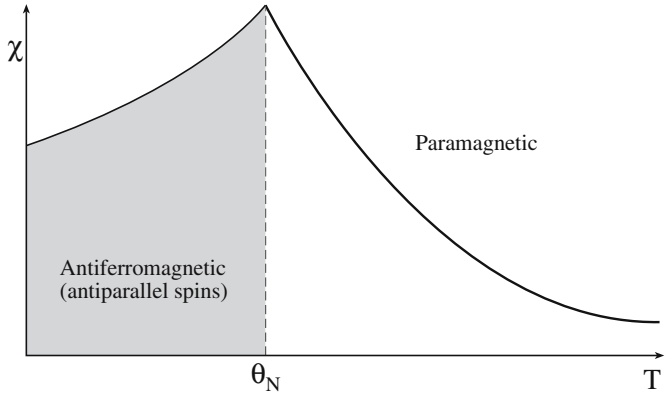

FIGURE 33.8 Schematic showing how χ varies with T for an antiferromagnetic material. At θ_N it becomes paramagnetic.

They all have the rocksalt (NaCl) structure and magnetic dipoles on adjacent {111} planes are antiparallel. The magnetic interaction between the cations occurs indirectly through the oxygen ions and is known as a "superexchange" interaction. Along <100> there is overlap of the Ni d_{z^2} orbitals and the O p_z orbital as illustrated in Figure 33.9. The Pauli exclusion principle governs the spin direction in the overlapping orbitals and, as a result, the adjacent Ni ions have opposed spins.

We have direct evidence of the orientation of the spin magnetic moments in antiferromagnetic materials from neutron diffraction studies. Neutrons have a magnetic dipole moment. In neutron diffraction the neutron beam is responding not only to atom positions but also to their magnetic moments. (X-rays give us information on atom positions and electron distribution.) Above θ_N, the neutron diffraction pattern consists of reflections due to the periodic arrangement of the crystal structure. Below θ_N extra reflections appear in the pattern because the neutrons are "seeing" two sets of cations, with different magnetic moments. The magnetic unit cell is therefore twice the size of the crystallographic unit cell as shown in Figure 33.10.

Antiferromagnetism is not limited to oxides with a rocksalt structure. The following antiferromagnets have a corundum structure:

$$V_2O_3\ (\theta_N = 173\,\text{K})\ \ Ti_2O_3\ (\theta_N = 660\,\text{K})$$
$$\alpha\text{-}Fe_2O_3\ (\theta_N = 950\,\text{K})$$

Although the ceramics we have mentioned so far in this section have no applications that use their magnetic

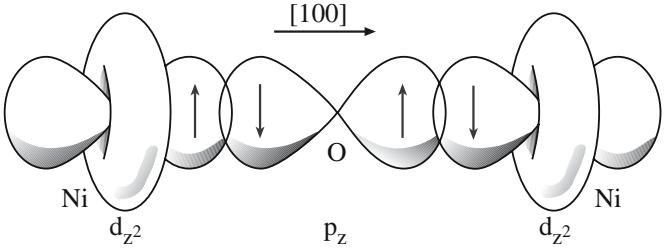

FIGURE 33.9 Overlap between Ni d_{z^2} orbitals and O p_z orbitals in Ni.

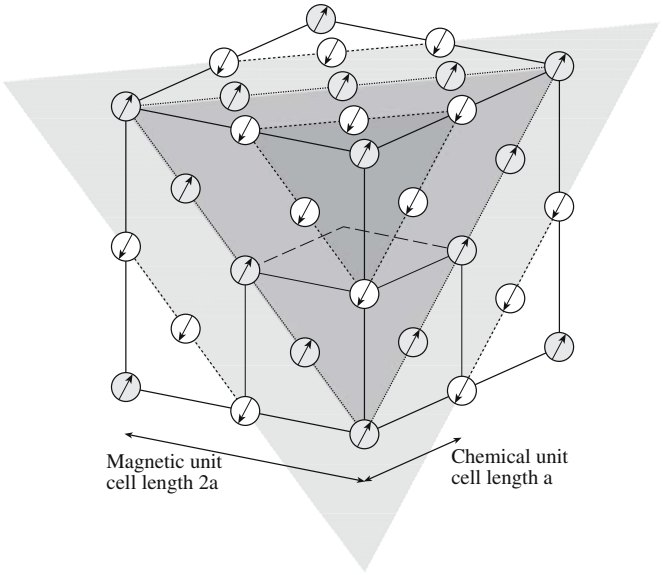

FIGURE 33.10 Comparison of structural and magnetic unit cells of NiO.

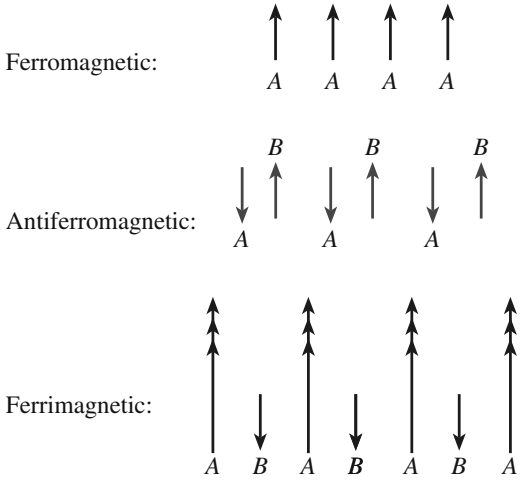

FIGURE 33.11 Schematic comparing dipole alignments in ferromagnetic, antiferromagnetic, and ferrimagnetic materials.

properties, there are manganate ceramics in the $La_{1-x}A_xMnO_3$ ($0 \le x \le 1$; A = Sr, Ca, Ba) system that are antiferromagnetic and exhibit colossal magnetoresistance (CMR). In CMR the resistance drops dramatically in an applied magnetic field. It is related to, but much greater than, giant magnetoresistance (GMR) found in multilayers of ferromagnetic and nonferromagnetic metals (e.g., 30 Co/Cu bilayers). In these structures there is an interaction between the ferromagnetic layers that can cause antiferromagnetic ordering of magnetic moments in adjacent layers. So individually each Co layer is ferromagnetic, but the multilayer structure is actually antiferromagnetic. The extent of the interaction depends on the thickness of the nonferromagnetic layer and *H*. All current hard disk drives make use of this technology.

The manganates have the layered perovskite structure similar to that found in the YBCO superconductor (see Section 7.16). This similarity is particularly interesting and may lead to increased understanding of both types of material. The nature of the interactions in the manganites is complicated. They show a metal–insulator transition and a ferromagnetic–antiferromagnetic transition associated with CMR.

33.11 FERRIMAGNETISM

In a ferrimagnet the magnetic moments of one type of ion on one type of lattice site in the crystal are aligned antiparallel to those of ions on another lattice site. Because the magnetic moments are not of the same magnitude they only partially cancel each other and the material has a net *M*. Ferrimagnetism has several similarities to ferromagnetism in that the cooperative alignment between magnetic dipoles leads to a net magnetic moment even in the absence of an applied field. Ferrimagnetism is lost above θ_c. The difference between ferromagnetism, antiferromagnetism, and ferrimagnetism in terms of the spin alignments is illustrated in Figure 33.11.

$ZnFe_2O_4$

In $ZnFe_2O_4$ [$Fe^{III}(Zn^{II}Fe^{III})O_4$] all the magnetic Fe^{3+} are on octahedral sites and are separated by a plane of O^{2-} ions. The material is antiferromagnetic because the superexchange interaction involving the two Fe^{3+} ions resembles that shown in Figure 33.9.

The easiest way to consider what happens in a ferrimagnet is to look at the prototypical ferromagnetic material, magnetite. Magnetite has an inverse spinel structure (Section 7.2). The formula can be written as $Fe^{III}(Fe^{II}Fe^{III})O_4$, i.e., in the classic spinel form AB_2O_4. The Fe^{2+} ions and half of the Fe^{3+} ions are in octahedral sites and the other half of the Fe^{3+} cations are in tetrahedral sites. The spins of the Fe ions on the octahedral sites are parallel, but of a different magnitude. The spins of the Fe ions on the tetrahedral sites are antiparallel to those in the octahedral sites. The situation is illustrated in Figure 33.12, which shows one-eighth of the magnetite unit cell. The alignment of the spins is the result of an exchange interaction involving the O^{2-} ions. The antiparallel alignment of the Fe^{3+} ion in the octahedral site and the Fe^{3+} ion in the tetrahedral site is usually explained by a superexchange reaction similar to that used to explain antiferromagnetism.

A mechanism to account for the parallel spin alignment between the Fe^{3+} in the octahedral site and the octahedrally coordinated Fe^{2+} was proposed by Zener and is called the "double exchange" mechanism. The idea is that an electron from the Fe^{2+} ion ($3d^6$) is transferred to the oxygen in the face-centered position of the subcell shown in Figure 33.12. At the same time there is transfer of an

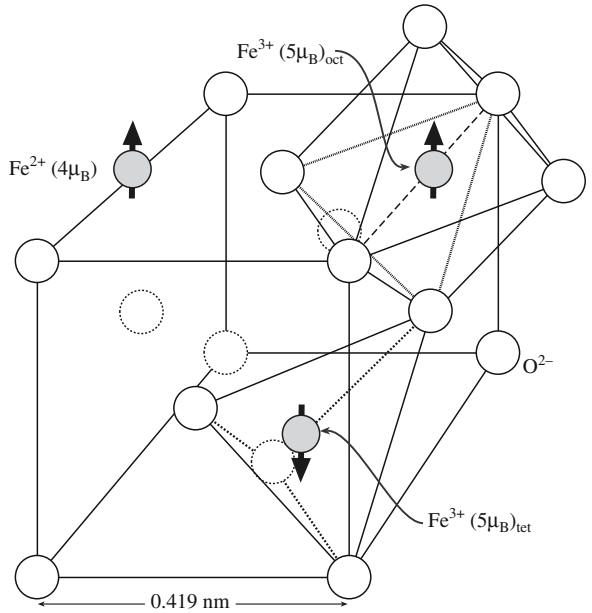

FIGURE 33.12 Subcell of magnetite showing the location of Fe ions and their spin moments.

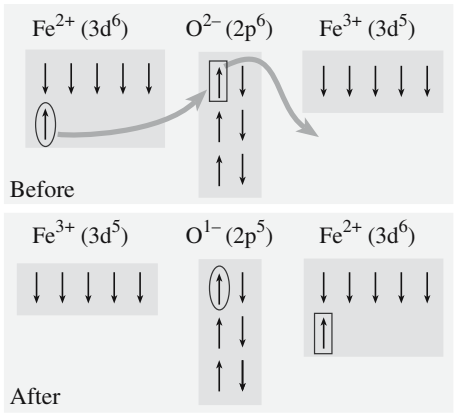

FIGURE 33.13 Illustration of the double exchange interaction in magnetite.

electron with parallel spin to the Fe^{3+} ion. The process is illustrated in Figure 33.13 and shares similarities with the electron-hopping model of conduction in transition metal oxides. (Note: a requirement of Zener's model is that the cations have different charges.)

Ferrimagnetic ceramics have the spinel (almost exclusively inverse), the garnet, or the magnetoplumbite structure. Table 33.6 lists some examples of ferrimagnetic spinels and their properties. The magnetic moments in this table were calculated taking account of only the number of unpaired 3d electrons; the units are Bohr magnetons and the minus sign denotes an antiferromagnetic coupling.

The most important and widely studied magnetic garnet is yttrium–iron garnet (YIG), which has the formula $Y_3Fe_2(FeO_4)_3$ [remember garnet is $Ca_3Al_2(SiO_4)_3$]. We can write the formula of YIG as $Y_3^cFe_2^aFe_3^dO_{12}$ where the superscripts refer to the type of lattice site occupied by each cation. The cell shown in Figure 33.14 is actually one of the eight subcells that form the YIG unit cell, which contains 160 atoms. In the subcell the *a* ions are in a body-centered cubic (bcc) type arrangement with the

TABLE 33.6 Magnetic Properties of Several Ferrimagnetic Ceramics

			Calculated moments			
Material	θ_c *(K)*	B_{sat} *(T) at RT*	*T site*	*O site*	*Net*	*Experimental*
Spinel ferrites [$AO \cdot B_2O_3$]						
$Fe^{3+}[Cu^{2+}Fe^{3+}]O_4$	728	0.20	−5	1.73 + 5	1	1.30
$Fe^{3+}[Ni^{2+}Fe^{3+}]O_4$	858	0.34	−5	2 + 5	2	2.40
$Fe^{3+}[Co^{2+}Fe^{3+}]O_4$	1020	0.50	−5	3 + 5	3	3.70–3.90
$Fe^{3+}[Fe^{2+}Fe^{3+}]O_4$	858	0.60	−5	4 + 5	4	4.10
$Fe^{3+}[Mn^{2+}Fe^{3+}]O_4$	573	0.51	−5	5 + 5	5	4.60–5.0
$Fe^{3+}[Li_{0.5}Fe_{1.5}]O_4$	943		−5	0 + 0.75		2.60
$Mg_{0.1}Fe_{0.9}[Mg_{0.9}Fe_{1.1}]O_4$	713	0.14	0–4.5	0 + 5.5	1	1.10
Hexagonal ferrites						
$BaO:6Fe_2O_3$	723	0.48				1.10
$SrO:6Fe_2O_3$	723	0.48				1.10
$Y_2O_3:5Fe_2O_3$	560	0.16				5.00
$BaO:9Fe_2O_3$	718	0.65				
Garnets						
$YIG\{Y_3\}[Fe_2]Fe_3O_{12}$	560	0.16			5	4.96
$(Gd_3)[Fe_2]Fe_3O_{12}$	560				16	15.20
Binary oxides						
EuO	69					6.8
CrO_2	386	0.49				2.00

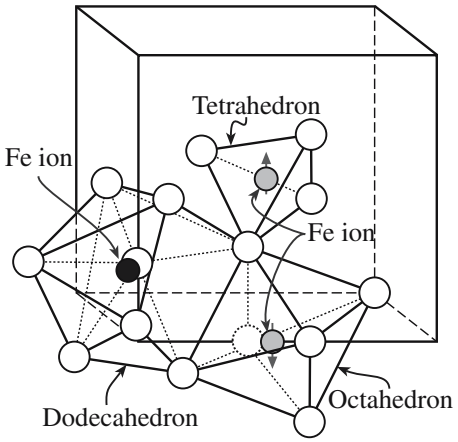

FIGURE 33.14 Structural units in a subcell of YIG. For clarity not all the atoms are shown and only one of each example of the polyhedra is shown.

c and *d* ions lying on the cube faces. Each *a* ion is in an octahedral site, each *c* ion is on a dodecahedral site, and each *d* ion is on a tetrahedral site as illustrated in Figure 33.14.

The net magnetic moment in YIG, as in other ferrimagnetic ceramics, arises from an uneven contribution from antiparallel spins; the magnetic moments of the *a* and *d* ions are aligned antiparallel as are those of the *c* and *d* ions. For every two Fe^{3+} on a sites, there are three Fe^{3+} ions on *d* sites giving a measured magnetic moment of ~5 μ_B.

The mineral magnetoplumbite has the approximate composition $PbFe_{7.5}Mn_{3.5}Al_{0.5}Ti_{0.5}O_{19}$. The commercially important ferrimagnetic ceramic barium hexaferrite ($BaO \cdot 6Fe_2O_3$) is isostructural with magnetoplumbite. A schematic of the crystal structure of $BaO \cdot 6Fe_2O_3$ is shown in Figure 33.15. The hexagonal unit cell is very large and contains 64 atoms. Magnetization is easiest along the *c* axis. Also shown in Figure 33.15 is a simplified representation of the spin magnetic moments of the Fe^{3+} ions in $BaO \cdot 6Fe_2O_3$. The actual arrangements are more complicated.

There is a range of hexagonal ferrimagnetic ceramics containing BaO. These are usually classified based on their chemical formula:

- M-type compounds, $(MO)(Fe_2O_3)_6$, e.g., $(BaO)(Fe_2O_3)_6$
- W-type compounds, $(BaO)(MO)_2(Fe_2O_3)_8$ or M_2W, e.g., $(BaO)(CoO)_2(Fe_2O_3)_8$
- Y-type compounds, $(BaO)_2(MO)_2(Fe_2O_3)_6$ or M_2Y, e.g., $(BaO)_2(MnO)_2(Fe_2O_3)_6$
- Z-type compounds, $(BaO)_3(MO)_2(Fe_2O_3)_{12}$ or M_2Z, e.g., $(BaO)_3(MgO)_2(Fe_2O_3)_{12}$

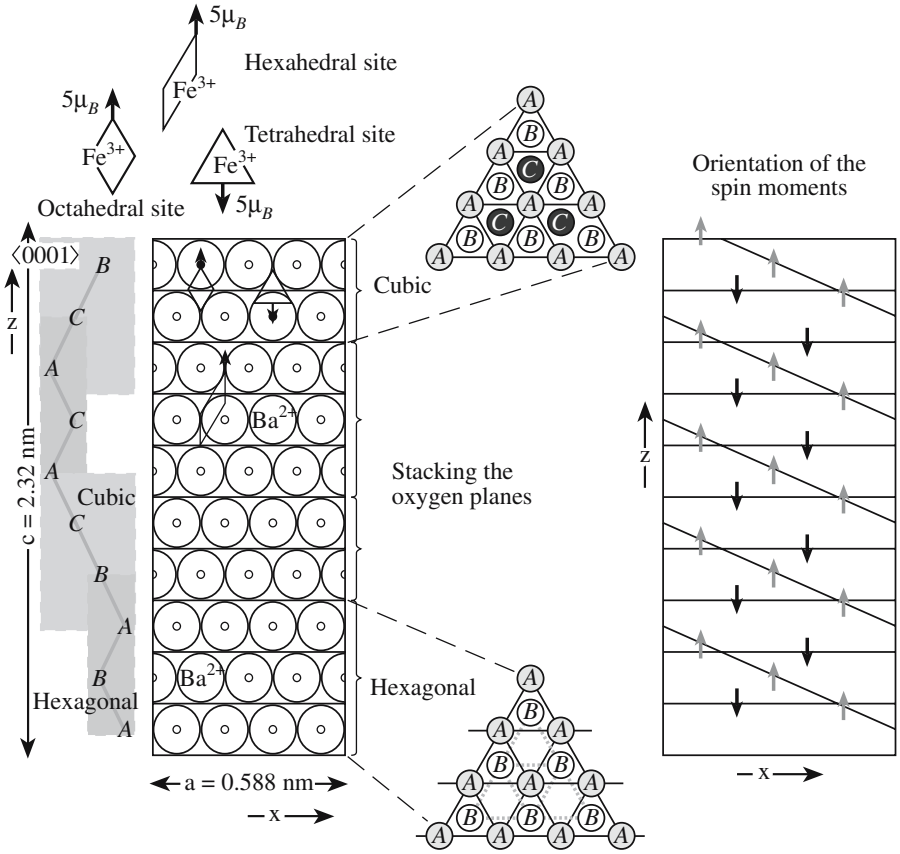

FIGURE 33.15 Schematic of the barium ferrite crystal structure showing the structural units and the magnetization directions.

TABLE 33.7 Magnetic Properties of Fe in Magnetic Ceramics

Ion	*Number*	*Site*	*Spin direction*	*Ion moment (μB)*	*Total moment (μB)*
Fe^{2+}	1	Octahedral	↑	4	4
Fe^{3+}	1	Octahedral	↑	5	5
Fe^{3+}	1	Tetrahedral	↓	5	−5

- X-type compounds, $(BaO)_2(MO)_2(Fe_2O_3)_{14}$ or M_2X, e.g., $(BaO)_2(FeO)_2(Fe_2O_3)_{14}$
- U-type compounds, $(BaO)_4(MO)_2(Fe_2O_3)1_8$ or M_2U, e.g., $(BaO)_4(ZnO)_2(Fe_2O_3)1_8$

33.12 ESTIMATING THE MAGNETIZATION OF FERRIMAGNETS

We can estimate saturation values of M and B by knowing the crystal structure and lattice parameter of the material and the orientation of the spin magnetic moments. We will illustrate this approach for magnetite. The magnetic moments of each type of ion are summarized in Table 33.7. The Fe^{3+} ions interact antiferromagnetically and the net magnetic moment is due only to the Fe^{2+} ions. Using Eq. Box 33.3 we can calculate the magnetic moment of an Fe^{2+} ion as $4.9\,\mu_B$. There are eight Fe^{2+} ions per unit cell so the total magnetic moment per cell is $8 \times 4.9 = 39.2\,\mu_B$.

DOMAIN WALL

Typically the domain wall has a thickness of about 100 nm and an energy of ~10^{-3} J/m^2.

M is therefore

$$39.2\ [\mu_B] \times 9.27 \times 10^{-24}\ [A{\cdot}m^2\ \mu_B^{-1}]/(0.837 \times 10^{-9}\ [m])^3 = 6.17 \times 10^5\ A/m$$

which is in fairly good agreement with the measured value of 5.3×10^{-5} A/m.

B is

$$B_S = \mu_0 M_s = 4\pi \times 10^{-7} \times 6.17 \times 10^5 = 0.78\ T$$

This value is close to the measured value of 0.6 T.

An interesting characteristic of both these values is that if the classical value of the spin magnetic moment is taken for Fe^{2+}, i.e., $4\,\mu_B$, then both M and B are closer to the measured values, even though for isolated cations Eq. Box 33.3 provides much better agreement with the experimental data. The reason for this discrepancy is not obvious.

33.13 MAGNETIC DOMAINS AND BLOCH WALLS

A ferromagnetic or a ferrimagnetic material is divided into many small regions or domains. Pierre Weiss was the first to recognize the presence of magnetic domains and therefore they are often named after him. Within each domain the direction of magnetization is the same. When the material is in its unmagnetized state the net magnetization is zero, i.e., there are as many domains magnetized in one direction as there are in the antiparallel direction. This situation is illustrated for several different domain structures in Figure 33.16. The energy of the material is lowered when the domains are smaller. For the configurations shown in Figure 33.16 the overall energy decreases from left to right. The triangular domains are called closure domains and complete the magnetic flux path with the solid; this also lowers the overall energy.

In the boundary region between the different domains there is a gradual change in magnetic dipole orientation as illustrated in Figure 33.17. The boundary regions are known as domain walls or Bloch walls after the man who did much of the early work on this subject. The thickness of the domain wall is a tradeoff between the requirement for a small angle between adjacent spins, which would necessitate a thick wall, and the tendency for the magnetic dipoles to be aligned with a specific crystallographic orientation, requiring a thin wall.

There is also a domain structure in antiferromagnetic materials, with wall separating each domain:

- In S walls the magnetization direction is rotated across the wall.
- In T walls there is a change in orientation characteristic of twinning.

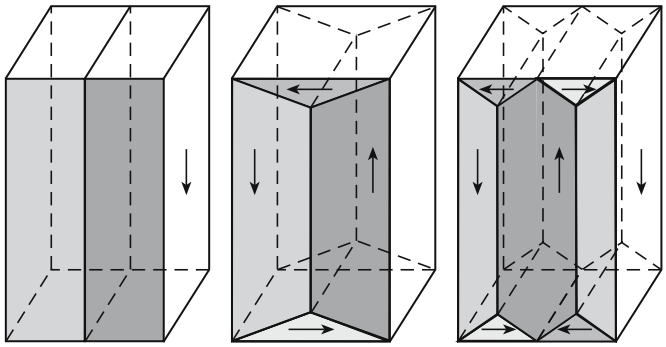

FIGURE 33.16 Examples of domain structures, each having zero net magnetization.

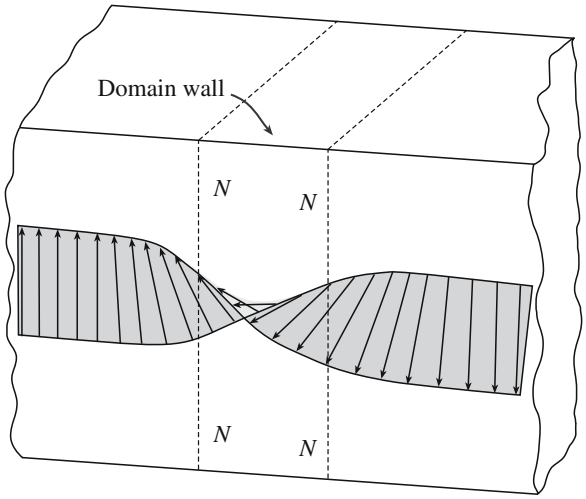

FIGURE 33.17 Change in magnetic dipole orientation through a domain wall. All moments lie in the plane of the wall.

33.14 IMAGING MAGNETIC DOMAINS

There are many different ways to image magnetic domain structures in a material. All the "microscopy" techniques we described in Chapter 10 can be used, although, in some cases, deviations from the usual operating procedure are necessary to obtain the desired images. It is also possible to use X-ray topography to study magnetic domains. In this section, we will briefly describe three techniques: the oldest, one of the newest, and the trickiest.

Visible Light Microscopy (VLM)

Examination of a magnetic material by simple VLM will not reveal any information about the domain structure because the direction of magnetization does not change the appearance of the surface in any way. Transmitted light requires that the specimens are transparent and so very thin (<0.1 μm) samples must be used. The first approach, known as the Bitter technique, "decorates" the domain boundaries with magnetic particles suspended in a liquid. The particles are attracted to where the domain boundaries intersect the surface and this allows the domain pattern to be observed. The Bitter technique is applicable to all types of magnetic material, but specimen preparation is important to avoid introducing surface strains that can distort the domain structure. A Bitter pattern obtained in the hexagonal ferrite $Co_2Ba_2Fe_{28}O_{46}$ is shown in Figure 33.18.

An alternative means of observing magnetic domain structures in the VLM is to use polarized light. Domains magnetized in opposite directions will rotate the plane of polarization in opposite senses. Using an appropriate analyzer it is possible to vary the intensity of the light coming from each domain and produce corresponding intensity changes in the image. The effect of M on the transmitted light intensity is called the Faraday effect. The Faraday effect in a thin film of a substituted YIG, $(BaTb)_3(FeGa)_5O_{12}$, is shown in Figure 33.19.

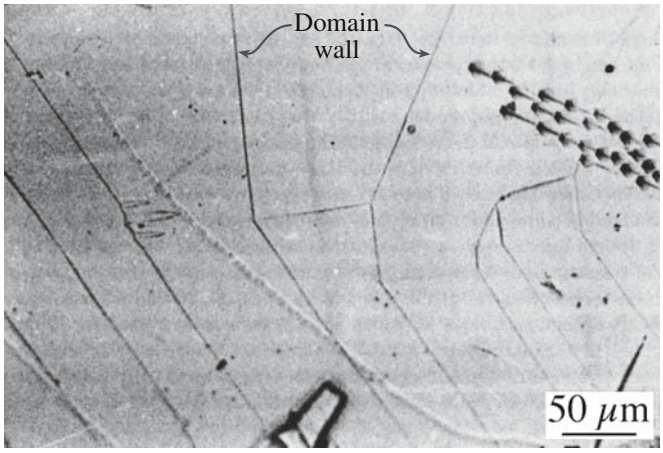

FIGURE 33.18 Magnetic domains on the basal surface of a hexagonal ferrite, $Co_2Ba_2Fe_{28}O_{46}$, revealed by the Bitter technique.

The effect of M on the reflected light intensity is known as the Kerr effect. The polar Kerr effect refers to a situation in which the sample has a component of M normal to the surface and normal incidence illumination is used. The longitudinal Kerr effect is used when M is parallel to the surface and the illumination is oblique.

Magnetic Force Microscopy (MFM)

Magnetic force microscopy is closely related to scanning tunneling microscopy (STM) and atomic force microscopy (AFM). In MFM the tip is coated with a ferromagnetic thin film that detects magnetic force variations on the sample surface. The tip is scanned over the surface of the sample (it does not actually touch) as in STM. Interactions between magnetic domains in the sample and the ferromagnetic coating result in a force on the tip, which

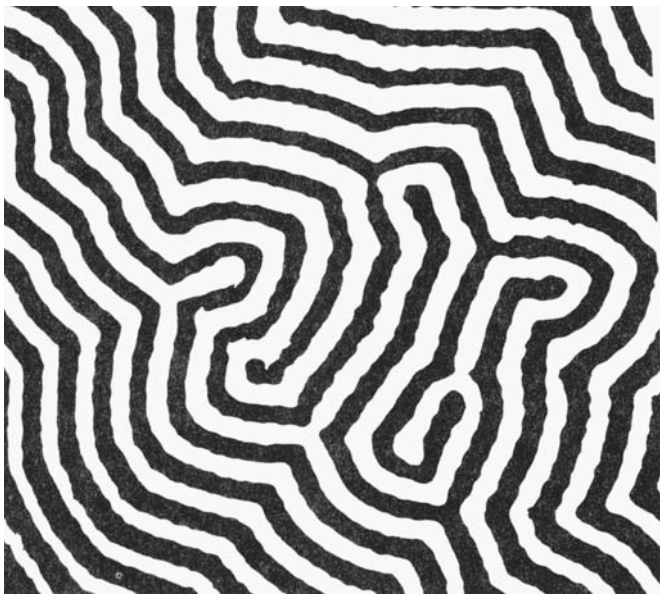

FIGURE 33.19 Domain pattern in a YIG thin film revealed by the Faraday effect. The stripes are 12 μm wide.

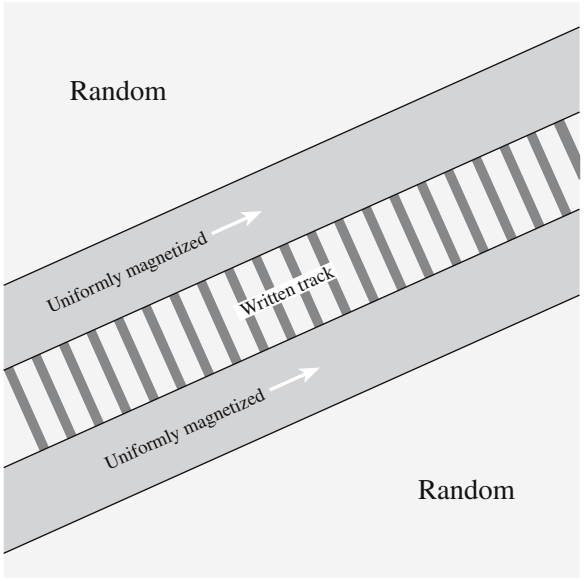

FIGURE 33.20 Schematic of MFM of a magnetized pattern on a hard drive.

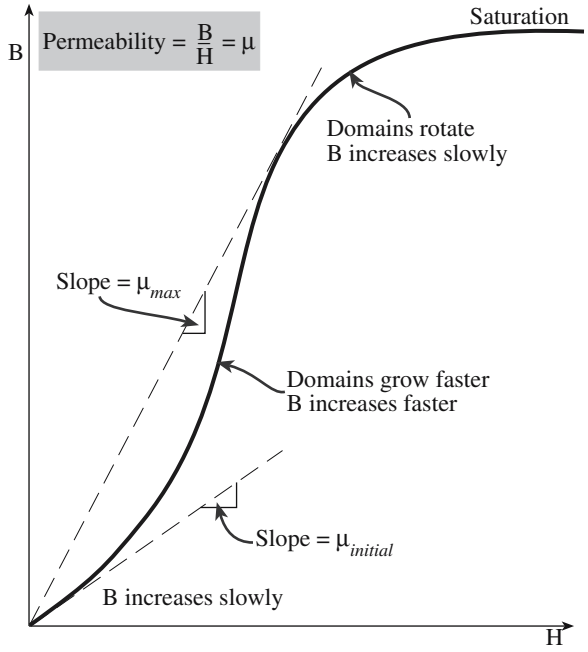

FIGURE 33.21 The effect of *H* on *B*. The ratio is μ.

depends upon the orientation of the domains. Different orientations produce a different force and this is how the different magnetized regions can be determined. Figure 33.20 illustrates how an MFM image of a magnetic tape would appear. The bright and dark stripes in the center of the image are regions where the direction of magnetization is different.

Transmission Electron Microscopy (TEM)

Because electrons are charged they experience a force—the Lorentz force—as they move through a magnetic field. This force causes them to be deflected by a small angle. The deflections are in different directions in different domains. The domain walls cannot be imaged under normal bright-field imaging conditions but they can be seen by either underfocusing or overfocusing the image (Fresnel images) or by displacing the objective aperture (Foucault images).

33.15 MOTION OF DOMAIN WALLS AND HYSTERESIS LOOPS

When an external magnetic field is applied to a ferromagnetic or ferrimagnetic material the domain boundaries begin to move. They move in such a way that domains in which the magnetization direction is aligned with *H* grow at the expense of the unaligned domains. The change in *B* with *H* is shown in Figure 33.21. Initially the movement of the domain walls is reversible and *B* increases only slightly with increasing *H*. As the field increases the favorably oriented domains grow more easily and μ increases. At very large *H* the unaligned domains will rotate and saturation will be reached in which all the domains are aligned in the same direction.

When the field is removed, there is a resistance to domain wall motion preventing reorientation of the domains. As a result there is a residual magnetization, known as remanence (B_r), and the material acts as a permanent magnet.

If *H* is then applied in a direction opposite to what was originally used then domains grow with an alignment in the new direction. A certain field, called the coercive field, H_c, is needed to completely randomize the domains. Further increases in *H* eventually align the domains to saturation in the new direction. The behavior of a ferromagnetic or a ferrimagnetic material in an alternating magnetic field is shown in Figure 33.22. The size of the

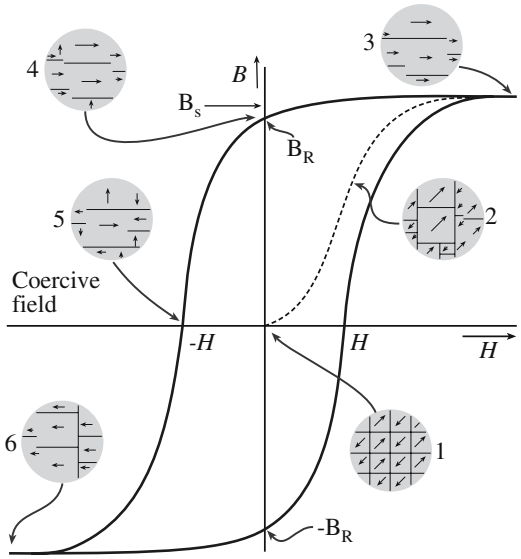

FIGURE 33.22 The variation of *B* as *H* alternates. The insets illustrate the domain structure at various points along the hysteresis curve.

TABLE 33.8 Classes of Magnetic Ceramic

Structure	*Composition*	*Applications*
Spinel (cubic ferrites)	1 MeO : 1Fe_2O_3 MeO = transition metal oxide, e.g., Ni,Co, Mn, Zn	Soft magnets
Garnet (rare earth ferrites)	3 Me_2O_3 : 5Fe_2O_3 Me_2O_3 = rare earth metal oxide, e.g., Y_2O_3, Gd_2O_3	Microwave devices
Magnetoplumbite (hexagonal ferrites)	1 MeO : 6Fe_2O_3 MeO = divalent metal oxide from group IIA; e.g., BaO, CaO, SrO	Hard magnets

hysteresis loop, i.e., the values of B_r and H_c, vary from material to material.

- When H_c is small (typically $<10^3$ A/m) the material is a *soft* magnet.
- When H_c is large (typically $>>10^3$ A/m) the material is a *hard* magnet.

Hard and soft do not have any connection to the mechanical properties of the material. There are examples of metals and ceramics that exhibit hard and soft behavior.

33.16 HARD AND SOFT FERRITES

The important ferrimagnetic ceramics form three groups depending on their crystal structures as summarized in Table 33.8. When we are considering possible applications it is more useful, at least to the engineers who are designing and building magnetic components, to specify the materials as hard or soft. These designations, as mentioned in Section 33.15, are based on the size of the *B–H* hysteresis loop, i.e., on the difficulty in reversing the direction of magnetization for the material. Hysteresis loops for hard and soft magnetic materials are compared schematically in Figure 33.23.

Convention: magnetic oxides that contain Fe^{3+} ions are called ferrites. This terminology does not distinguish between the crystal structures; do not confuse it with the chemical name. We often say that ferrites contain Fe_2O_3 as a principal component.

Hard Ferrites

Hard ferrites, which are used to fabricate permanent magnets, must have large

- H_c
- B_r

To satisfy these requirements, it is necessary to use materials with crystal structures that exhibit a large magnetic anisotropy and to prevent the growth and rotation of magnetic domains (by, for example, controlling the grain size so that each grain becomes a single domain). Barium ferrite and oxides with a magnetoplumbite structure are the preferred choice.

Philips introduced ferrite magnets commercially in 1952 under the trade name "Ferroxdure." About 550,000 t of hard ferrites are produced annually (>95% of the hard magnet market). This is more than metallic magnets. There are a number of reasons why ferrite magnets are commercially so important, not least of which is that the raw materials are relatively cheap and widely available and the manufacturing processes are simple.

Hard ferrite magnets are found in the following:

- Starter motors in automobiles
- Loudspeakers
- Rotors for cycle dynamos
- Windscreen wiper motors
- Mixed with a flexible polymer in door-catches and decorative magnets for refrigerators

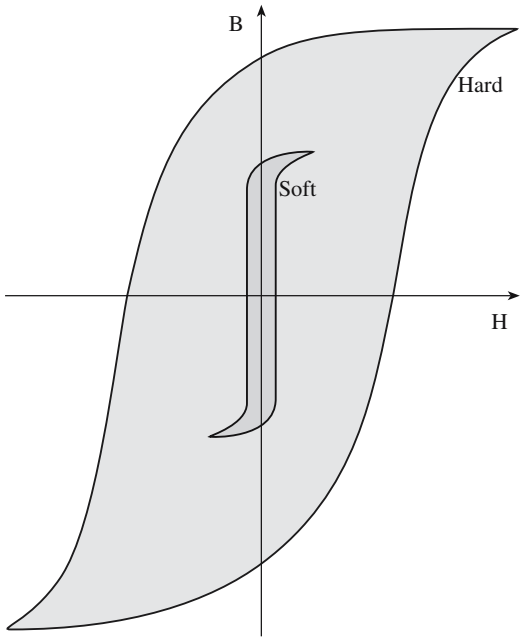

FIGURE 33.23 Comparison of the size and shape of hysteresis loops for hard and soft magnets.

TABLE 33.9 Properties of Several Hard Magnets

Material	*Composition (wt%)*	B_r *(T)*	H_c *(A-turn m^{-1})*	$(BH)_{max}$ *(kJ/m^3)*	θ_c *(°C)*	ρ *(Ω·m)*
Tungsten steel	92.8 Fe 6 W 0.5 Cr 0.7 C	0.95	5,900	2.6	760	3.0×10^{-7}
Cunife	20 Fe 20 Ni 60 Cu	0.54	44,000	12	410	1.8×10^{-7}
Sintered alnico	34 Fe 7 Al 15 Ni 35 Co 4 Cu 5 Ti	0.76	125,000	36	860	—
Sintered ferrite	$BaO–6Fe_2O_3$	0.32	240,000	20	450	~10^4
Cobalt rare earth	$SmCo_5$	0.92	720,000	170	725	5.0×10^{-7}
Sintered neodymium–iron–boron	$Nd_2Fe_{14}B$	1.16	848,000	255	310	1.6×10^{-6}

- DC motors in fuel pumps
- Household appliances such as electric shavers, food mixers, and coffee grinders
- Magnetic strips on credit cards, ATM cards, etc.

Table 33.9 compares some of the important properties of hard ferrites with hard metal alloy magnets such as alnico and high-energy ($BH \geq 80\,kJ/m^3$) rare earth magnets such $SmCo_5$.

Soft Ferrites

The prime requirement for a soft ferrite is that a high M can be produced using a small H. This means that soft ferrites should have

- High μ
- Low H_c

Soft ferrites therefore have narrow hysteresis loops. During changes in field direction the domains are rapidly and easily realigned with the changing magnetic field. Consequently, domain wall motion and/or magnetization rotation must be easy. Domain wall motion is particularly sensitive to the microstructure of the material and characteristics such as grain size and grain-boundary structure, the presence of inclusions or pores within the grains, impurity levels, and stresses all reduce domain wall motion. Porosity is particularly common in many sintered ceramics and ferrites are certainly no exception. As a result magnetization rotation plays an important role in reaching B_s. Soft ferrites should also have high electrical resistivities (not a problem for most ceramics!) because this limits eddy current losses.

Soft ferrites are generally used in applications in which the direction of H is frequently changing such as high-frequency inductors and transformers and magnetic elements in microwave components. There are plenty of household examples in which soft ferrites are used:

- Magnetic recording and data storage media
- Transformer cores in telephones
- Numerous applications in radios and televisions, such as line transformers, deflection coils, tuners, and rod antennas

Table 33.10 compares some of the relevant properties of metal and ceramic soft magnets. Spinel ferrites based upon the $(Mn,Zn,Fe)O_4$ system are examples of commercially important soft magnets. The market for soft ferrites is about 50,000 t per year. These are usually marketed under the trade name *Ferroxcube*.

TABLE 33.10 Properties of Several Soft Magnets

Material	*Composition (wt%)*	μ_i	B_s *(T)*	*Hysteresis loss/cycle (J/m^3)*	ρ *(Ω·m)*
Iron	99.95 Fe	150	2.14	270	1.0×10^{-7}
Silicon-iron (oriented)	97 Fe, 3 Si	1,400	2.01	40	4.7×10^{-7}
45 Permalloy	55 Fe, 45 Ni	2,500	1.60	120	4.5×10^{-7}
Supermalloy	79 Ni, 15 Fe, 5 Mo, 0.5 Mn	75,000	0.80	—	6.0×10^{-7}
Ferroxcube A	48 $MnFe_2O_4$, 52 $ZnFe_2O_4$	1,400	0.33	~40	2,000
Ferroxcube B	36 $NiFe_2O_4$, 64 $ZnFe_2O_4$	650	0.36	~35	10^7

Garnets also tend to be soft magnets but are not as widely used as the cubic ferrites: they are more expensive. There was a great deal of interest in the late 1960s and 1970s in magnetic garnets for use in bubble memory. A magnetic bubble is a small (from about 0.05 μm up to 10 μm) cylindrical region, which has M in the opposite direction to H.

A bubble memory is nonvolatile, which means that once information is stored it remains even when the power is removed (just like current hard drives). Bubble memories used a thin layer (usually about 4 μm) of a magnetic garnet (a typical formulation being $Y_{2.6}Sm_{0.4}Ga_{1.2}Fe_{3.8}O_{12}$) deposited by liquid phase epitaxy onto a substrate of gadolinium gallium garnet (GGG). The strain induced by the lattice misfit and differences in the coefficient of thermal expansion between the two garnets resulted in an anisotropic axis normal to the film.

By the mid-1970s most of the large electronic companies were working on bubble memories and by the late 1970s there were several commercial products. By the 1980s the bubble memory market was dead. One of the reasons was the introduction of larger and faster hard drives.

33.17 MICROWAVE FERRITES

When a magnetic field is applied to a spinning electron it precesses around the field direction in much the same way that a spinning top precesses around the direction of a gravitational field. In ferromagnetic and ferrimagnetic materials the electron spins are coupled and the magnetization vector, ***M***, will precess around the field direction as shown in Figure 33.24. The interaction between electromagnetic waves and the precessing spin magnetic moments in the ferrite has been used to make waveguides for microwaves. Microwaves are electromagnetic radiation with frequencies in the range of 1–300 GHz (λ = 30 cm to 3 mm). As they travel along the waveguide their behavior is modified.

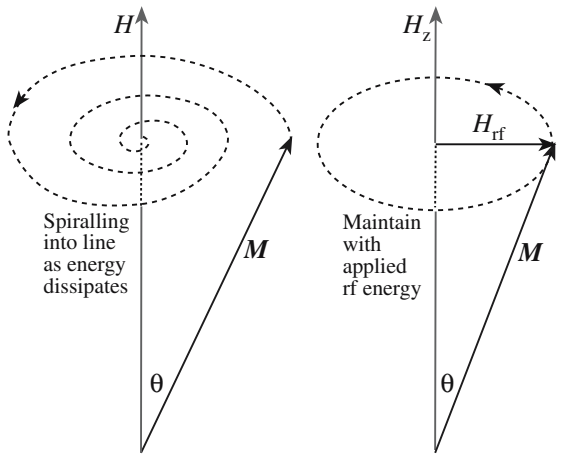

FIGURE 33.24 Illustration of the precessional motion of the magnetization vector.

An important example is known as Faraday rotation, which involves the rotation of the plane of polarization of a plane wave as it travels through the waveguide. A plane-polarized wave is equivalent to two circularly polarized waves, polarized in opposite senses (i.e., a right-polarized and a left-polarized component). Each component interacts very differently with the precessing spins and encounters different permeabilities, which affect the velocities of the two waves. The left component is retarded relative to the right, causing a clockwise rotation of the plane of polarization.

The most direct application of Faraday rotation is to use waveguides in the same way that polarizers and analyzers are used in light optics: to accept or reject plane polarized waves.

There are several different types of microwave devices. Isolators allow transmission of microwave radiation in one direction (they are used to prevent unwanted reflected signals). Gyrators are used to rotate the plane of polarization. There are other, more complicated devices, such as phase shifters and circulators. Garnets are widely used in microwave engineering because their properties can be tailored for the specific application. A garnet that is currently used in radar phase shifters is $Y_{2.66}Gd_{0.34}Fe_{4.22}Al_{0.68}Mn_{0.09}O_{12}$.

Microwave ferrites are used in radar-absorbing paint, which is used to make planes such as the F-117 Nighthawk and the B-2 Spirit "stealthy."

33.18 DATA STORAGE AND RECORDING

Magnetic recording is a major technology for electronic information mass storage. Its presence is ubiquitous in audio and video cassette tapes, floppy disks, computer hard disks, credit cards, etc. The magnetic audio recorder was invented in 1898. Video recorders were first introduced in 1955 primarily for use by broadcasters before they became widely available for commercial use. Now magnetic recording equipment has spread to almost every household with sales exceeding $50 billion per year.

Magnetic recording materials such as magnetic tapes and floppy disks are collections of very fine magnetic particles supported on a flexible polymer such as polyethylene terephthalate (PET). The basic features of magnetic recording are illustrated in Figure 33.25. A minute part of the magnetic tape is magnetized by a signal from a magnetic head and data are stored in a form of the magnetization direction. The properties of the material used for this purpose are quite specific:

- H_c must be high enough to maintain magnetization but sufficiently low to allow stored data to be erased
- Chemically stable

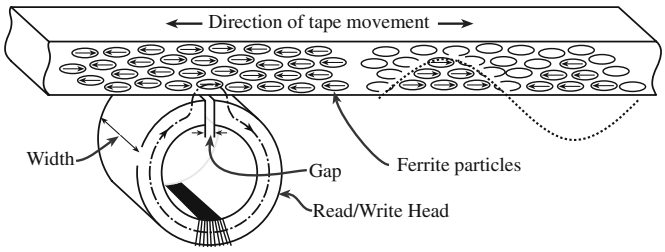

FIGURE 33.25 Illustration of the principal features of longitudinal recording.

- Small (<1 μm), uniformly distributed acicular particles
- Uniform distribution of particles
- Cheap

Three types of ceramic particles are currently used as magnetic media: γ-Fe_2O_3, Co-γ-Fe_2O_3, and CrO_2. Their properties are given in Table 33.11. Iron oxide particles were first used in magnetic recording in the 1930s and now account for 90% of this market. The standard method for making γ-Fe_2O_3 involves dehydrating goethite (α-FeOH) to hematite (α-Fe_2O_3) followed by reducing the hematite to magnetite (Fe_3O_4) and finally oxidizing the magnetite to maghemite (γ-Fe_2O_3).

Various experimental modifications have been made to the process over the years to produce γ-Fe_2O_3 particles that have the required shape and uniformity for use as magnetic media. The γ-Fe_2O_3 particles typically have lengths in the range of 100–700 nm and aspect ratios up to 10. H_c of γ-Fe_2O_3 is at the low end of the useful range for magnetic recording. As a result it is more useful at recording signals in the low frequency range. Cobalt-modified γ-Fe_2O_3 particles were developed to increase H_c. These particles were widely used in audiocassette tapes (before the advent of CDs and iPods) and also on some videocassette tapes. The reason for the higher H_c is not well understood.

The process for producing chromium dioxide (CrO_2) particles for magnetic media was developed by the DuPont Company in the 1960s. Because of the higher uniformity in size and shape of the particles CrO_2 tends to have a much higher H_c than γ-Fe_2O_3. This makes CrO_2 more suitable for high-density recording. It also has a high M giving a large range of response and thus a high quality of reproduction. The small particle size and the very uniform particle size distribution mean that CrO_2 tapes have much lower noise (less background hiss on audio tapes; less "snow" on video pictures). Chromium dioxide is widely used in tapes for videocassettes and for professional audiotapes. The drawbacks of CrO_2 are

- Low θ_c
- Toxicity
- It is abrasive to some types of recording head
- Magnetic properties degrade slowly with time

But the main drawback that prevented its more widespread use in audiotapes is that it is more expensive than γ-Fe_2O_3.

Ferrites can be used to store a considerable amount of information, but in many applications are being replaced by optical information storage such as CDs and DVDs.

Magnetic materials are used in the read and write heads of magnetic storage drives. The most significant change since the beginning of this technology and the use of conventional recording heads using magnetic inductance was the introduction of magnetoresistive (MR) and then GMR recording heads. These allowed data to be stored more densely and read more quickly. GMR is now used in most modern hard drives. Ceramic CMR materials may produce the next big change. In CMR resistance does not change by a few percent but by orders of magnitude. Applications for these materials are being developed.

The use of barium ferrite for high-density recording applications has been investigated because it is chemically stable and can have H_c ~480 kA/m. The hexagonal particles can, in principle, be oriented with their c axis normal to the tape surface as shown in Figure 33.26. This is known as a perpendicular medium and can give very high recording densities. Hexagonal ferrites are used in the magnetic strips on credit cards and ATM cards. In these applications we want the data to be permanent.

MAGHEMITE

The name *maghemite* was first suggested in 1927. It is a combination of the first syllables of *mag*netite, which has the same structure, and *hem*atite, which has the same composition.

TABLE 33.11 Physical and Magnetic Properties of Magnetic Particles

Magnetic particle	*Particle length (μm)*	*Aspect ratio*	*Specific surface area (m^2/g)*	H_c *(kA/m)*	B_s *(T)*	θ_c *(°C)*
γ-Fe_2O_3	0.3–0.6	10	20–30	20–32	0.5	675
Co–γ-Fe_2O_3	0.3–0.4	10	20–30	30–70	0.5	400
CrO_2	0.2–0.7	10–20	24–40	30–50	0.5	113
Fe (metal)	0.2–0.4	~6	40–50	75–130	2.0	770

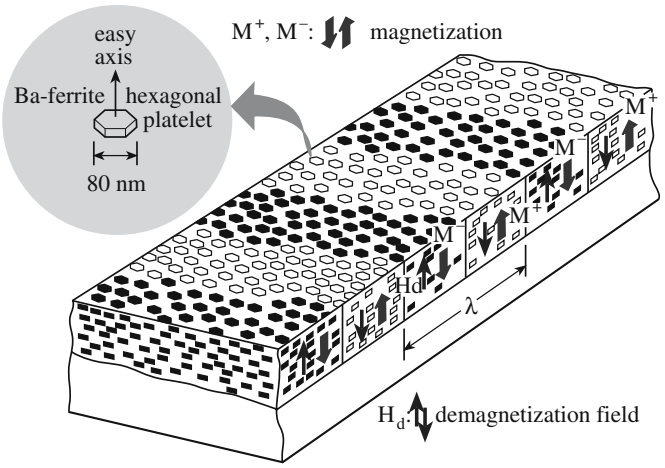

FIGURE 33.26 The principle of perpendicular recording.

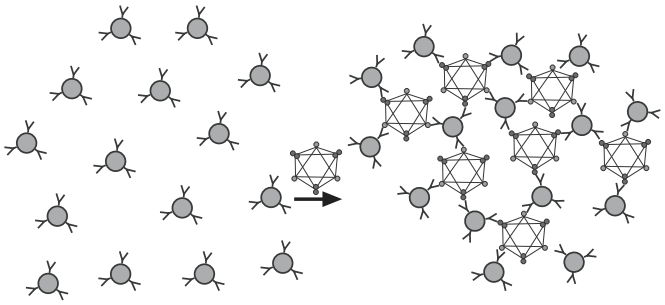

FIGURE 33.27 Diagram of a viral-induced nanoassembly of magnetic nanoparticles.

33.19 MAGNETIC NANOPARTICLES

Magnetic ceramic nanoparticles are becoming of increasing interest in a number of areas. One of these areas is using them for the location and detection of viruses: a viral nanosensor. The approach is illustrated in Figure 33.27. Iron oxide particles (~50 nm in diameter) with a dextran coating are covered with antibodies. The antibodies are chosen for a specific virus (e.g., herpes simplex virus or adenovirus). When these specially coated nanoparticles are then exposed to the virus they will form clusters that would be large enough to be visible on a nuclear magnetic resonance (NMR) or magnetic resonance imaging (MRI) scan. This approach has already been demonstrated in the laboratory using viral particles in solution. The idea is that it might eventually be used to detect viruses in human body fluid or tissue.

CHAPTER SUMMARY

In this chapter we described the different magnetic properties of ceramics. Most ceramics are diamagnetic, a very weak and commercially unimportant property. The most important magnetic properties of ceramics arise because of the presence of unpaired electron spins, primarily in the 3d orbitals of Fe. Ferrites, a class of magnetic ceramics containing Fe_2O_3, are used in a wide variety of applications, and their production constitutes a multibillion dollar industry. Ferrites can be classified according to their structure, and there are three structural types: spinel or cubic ferrites, garnets, and hexagonal ferrites. The cubic ferrites, of which γ-Fe_2O_3 (maghemite) is the most ubiquitous example, are soft magnetic materials and hence the direction of magnetization can be relatively easily changed in an alternating magnetic field. Maghemite was used extensively in audiotapes and floppy disks (which have now largely been replaced by iPods and CDs). The magnetic garnets are used in microwave applications including ingredients on radar-absorbing paint for stealthy airplanes. The hexagonal ferrites, such as $BaO \cdot 6Fe_2O_3$, are hard or permanent magnetic materials. They are more difficult to demagnetize. Barium hexaferrite is used in many applications from small electric motors in automobiles, to the magnetic seal on a refrigerator, to the magnetic strip on credit cards. Manganates, which have the technologically important layered perovskite structure, exhibit a property called colossal magnetoresistance and offer potential in a number of technologies from read/write heads in magnetic recording, sensors, and spin-polarized electronics.

PEOPLE IN HISTORY

Bitter, Francis (1902–1967) was born in Weehawken, New Jersey. In 1931 he discovered a method for visualizing magnetic domains. In 1934 he joined the Department of Mining and Metallurgy at M.I.T (where he spent most of his career) and helped establish a high field magnet laboratory. During WW II, he worked in England on methods to demagnetize German mines in the English Channel. His work after the war led to the establishment of the National Magnet Laboratory, which after his death was renamed the Francis Bitter National Magnet Laboratory.

Bloch, Felix (1905–1983) was born in Zurich, Switzerland. He received his Ph.D. in 1928 from the University of Leipzig where he worked with Heisenberg. Upon Hitler's rise to power Bloch left Europe and moved to the United States where he accepted a position at Stanford University. He was awarded the 1952 Nobel Prize in Physics for the development of the NMR technique.

Curie, Pierre (1859–1906) was born in Paris. In 1895 he obtained his Doctor of Science degree and was appointed Professor of Physics at the Sorbonne. In his early studies on crystallography, together with his brother Jacques, he discovered the piezoelectric effect. Later, he turned his attention to magnetism and showed that the magnetic properties of a given substance change at a certain temperature (the Curie temperature). He was awarded the Nobel Prize in physics in 1903 (together with his wife Marie) for their work in radioactivity. On April 19, 1906 he was killed in a street accident in Paris.

GMR was discovered in 1988; CMR was discovered in 1993.

Josephson, Brian David (1940–) was born in Cardiff, Wales and discovered the Josephson effect while a 22-year-old graduate student at the University of Cambridge. He won the Nobel Prize in physics in 1973 for his discovery.

Lenz (pronounced *lents*), Heinrich Friedrich Emil (1804–1865) was born in Dorpat, Russian Empire (now Tartu, Estonia) and formulated his eponymous law of electromagnetism in 1833. He participated in a round-the-world expedition in 1823–1826 and made extremely accurate measurements of the properties of seawater.

London, Fritz (1900–1954) was born in Breslau, Germany (now Wroclaw, Poland). He fled Nazi Germany in 1933 and came to the United States in 1939 where he became naturalized in 1945. Together with his younger brother Heinz he formulated the London equations of superconductivity.

Meissner, Walther (1882–1974) and his graduate student Robert Ochsenfeld (1901–1993), both Germans working in Berlin, discovered in 1933 that a superconducting material repels a magnetic field—behaving as a perfect diamagnet. The effect became known as the Meissner (or Meissner–Ochsenfeld) effect.

Oersted, Hans Christian (1777–1851) was a Danish physicist and philosopher. He demonstrated the fundamental relationship between electricity and magnetism on July 21, 1820 during a lecture on electricity at the University of Copenhagen. He showed that a compass needle is deflected when a wire carrying an electric current is placed near it. In addition to his work in electricity and magnetism, Oersted was the first to prepare pure metallic aluminum (1825).

Weiss, Pierre Ernest (1865–1940) was born in Mulhouse in the Alsace region of eastern France. He proposed the domain theory of ferromagnetism in 1907 while he was working at the Polytechnic Institute in Zurich.

GENERAL REFERENCES

Cullity, B.D. (1972) *Introduction to Magnetic Materials*, Addison-Wesley, Reading MA. A standard, but now dated, text on magnetism.

Jakubovics, J.P. (1994) *Magnetism and Magnetic Materials*, The Institute of Materials, London. A good overview (and brief), it includes more methods for measuring magnetic susceptibility.

Kittel, C. (1986) *Introduction to Solid State Physics*, 6th edition, Wiley, New York. Chapter 14 describes diamagnetism and paramagnetism and Chapter 15 describes ferromagnetism and antiferromagnetism. The approach is quite mathematical and goes deeper into the fundamentals than we do.

Moulson, A.J. and Herbert, J.M. (1990) *Electroceramics*, Chapman & Hall, London. A very good text on this topic.

Owens, F.J. and Poole, C.P., Jr. (1996) *The New Superconductors*, Plenum Press, New York. A gentle introduction to ceramic superconductors includes a very readable account of the flux lattice.

Purcell, E.M. (1985) *Electricity and Magnetism*, 2nd edition, McGraw-Hill, New York. An E&M reference. Purcell shared the 1952 Nobel Prize in physics with Bloch.

Standley, K.J. (1972) *Oxide Magnetic Materials*, 2nd edition, Clarendon Press, Oxford. A very useful reference on this topic. Described the structure of manganates before their commercial importance was realized.

SPECIFIC REFERENCES

Kato, Y. and Takei, T. (1932) Japanese patent 98,844. The first commercial applications of ferrites.

Néel, L. (1948) "Proprietes magnetiques des ferrites—ferrimagnetisme et antiferromagnetisme," *Ann. Phys.* **3**, 137. The original description of ferrimagnetism. Néel won the 1970 Nobel Prize in physics for his work on antiferromagnetism and ferrimagnetism.

Perez, J.M., Simeone, F.J., Saeki, Y., Josephson, L., and Weissleder, R. (2003) "Viral-induced self-assembly of magnetic nanoparticles allows the detection of viral particles in biological media," *J. Am. Chem. Soc.* **125**, 10192. Description of a viral nanosensor using iron oxide nanoparticles. This group is at Harvard Medical School.

Roth, W.L. (1960) "Neutron and optical studies of domains in NiO," *J. Appl. Phys.* **31**, 2000. The first description (and naming) of domain boundaries in antiferromagnets.

Shull, C.G. and Smart, J.S. (1949) "Detection of antiferromagnetism by neutron diffraction," *Phys. Rev.* **76**, 1256. The original neutron diffraction studies on antiferromagnetic materials.

Smit, J. and Wijn, H.P.J. (1959) *Ferrites*, Wiley, New York. More detailed description of magnetoplumbite ferrites.

Snoeck, J.L. (1947) *New Developments in Ferromagnetic Materials*, Elsevier, New York. The first major published study of ferrites.

Weiss, P. (1906) "The variation of ferromagnetism with temperature," *Compt. Rend.* **143**, 1136. Weiss domains.

Williams, D.B. and Carter, C.B. (1996) *Transmission Electron Microscopy: A Textbook for Materials Science*, Plenum, New York. The Lorentz technique is described on pp. 534–537.

Zener, C (1951) "Interaction between the d-shells in the transition metals," *Phys. Rev.* **81**, 440 and "Interaction between the d-shells in the transition metals 2: Ferromagnetic compounds of manganese with perovskite structure," *Phys. Rev.* **82**, 403. These two papers have been cited collectively almost 4000 times and describe the double exchange mechanism. Clarence Zener spent a short time (1940–1942) as an instructor at Washington State University when it was still known as Washington State College.

EXERCISES

33.1 Diamagnetism is present in all materials. Why do we not usually need to consider its contribution when we determine χ for a paramagnetic material using a Gouy balance?

33.2 You are given a sample of a ceramic powder that you believe to be paramagnetic. You have access to a Gouy balance. Explain how you would determine χ for your powder and what possible sources of error there might be.

33.3 In Section 33.4 we said that there are two general categories of magnetic behavior. Assign each of the five main types of magnetic response, diamagnetism, paramagnetism, ferromagnetism, antiferromagnetism, and ferrimagnetism, into one of the two categories. Explain briefly how you arrived at your assignments.

33.4 Al_2O_3, BeO, diamond, MgO, NaCl, and Si are all diamagnetic. Explain this observation.

33.5 You perform experiments using a Gouy balance using sintered rods of Al_2O_3, BeO, CeO_2, and TiO_2. What sign would you expect to obtain for χ for each material? Would you get a different result if you replaced the oxide with its corresponding metal?

33.6 How would the magnetic properties of magnetite change if it were a normal spinel?

33.7 Sketch the position of the atoms in the perovskite unit cell that you would expect for the CMR compound $La_{0.5}Ca_{0.5}MnO_3$.

33.8 The compounds in the $La_{1-x}A_xMnO_3$ system contain both Mn^{3+} and Mn^{4+} ions and are collectively called "manganites." Is the use of this term correct scientific usage or not? Briefly explain your answer.

33.9 Liquid phase epitaxy (LPE) was used for forming thin garnet films for magnetic bubble memories. Describe the basic principles behind this technique. Would sputtering or evaporation be good alternative techniques for such films? Explain how you arrived at your answer.

33.10 Compare the energy and width of domain boundaries with values for grain boundaries. Based on the values you obtain discuss the relative ease of movement of the two types of boundary.